Journal of Alloys and Compounds 509 (2011) 1322–1327

Contents lists available at ScienceDirect

Journal of Alloys and Compounds

journal homepage: www.elsevier.com/locate/jallcom

Effects of precipitator on the morphological, structural and electrochemical characteristics of $Li[Ni_{1/3}Co_{1/3}Mn_{1/3}]O_2$ prepared via carbonate coprecipitation

C. Deng[a,*], S. Zhang[b,**], L. Ma[a], Y.H. Sun[a], S.Y. Yang[b], B.L. Fu[b], F.L. Liu[b], Q. Wu[b]

[a] College of Chemistry and Chemical Engineering, Provincial Key Lab for Nano-Functionalized Materials and Excitated States, Harbin Normal University, Harbin 150025, Heilongjiang, China
[b] College of Material Science and Chemical Engineering, Harbin Engineering University, Harbin 150001, Heilongjiang, China

ARTICLE INFO

Article history:
Received 8 June 2010
Received in revised form
30 September 2010
Accepted 7 October 2010
Available online 15 October 2010

Keywords:
Cathode material
Carbonate coprecipitation
Precipitator
$Li[Ni_{1/3}Co_{1/3}Mn_{1/3}]O_2$
Lithium ion battery

ABSTRACT

Three precipitators, i.e. Na_2CO_3, $(NH_4)_2CO_3$ and NH_4HCO_3, are employed to prepare $Li[Ni_{1/3}Co_{1/3}Mn_{1/3}]O_2$ via the carbonate coprecipitation method. The effects of precipitator on the morphological, structural and electrochemical characteristics of the prepared samples are studied. The sample prepared by using Na_2CO_3 as precipitator has irregular particle shape and nonuniform particle size, while the sample prepared by using $(NH_4)_2CO_3$ as precipitator has spherical particle shape and uniform particle size. Among all the samples, the one prepared with $(NH_4)_2CO_3$ exhibits the best hexagonal layered structure, which results in its highest discharge capacity and best cycling performance. Therefore, precipitator plays an important role in the coprecipitation reaction and makes a great impact on the characteristics of $Li[Ni_{1/3}Co_{1/3}Mn_{1/3}]O_2$.

1. Introduction

Lithium ion batteries (LIB) have become an important power source for portable electronic devices, such as cellular phones and laptop computers [1,2]. $LiCoO_2$ has been widely used as the cathode material for commercial LIB because of its low irreversible capacity loss and good cycling performance. However, such disadvantages as the high cost, limited capacity and toxicity inhibit its further application in high power and price-sensitive fields, e.g. hybrid electric vehicles (HEV) [3–5]. Thus, extensive research has been carried out over the past ten years to find alternative materials with the low cost, long life and high capacity.

$Li[Ni_{1/3}Co_{1/3}Mn_{1/3}]O_2$, a special case of $Li[Ni_xCo_{1-2x}Mn_x]O_2$ system, has been considered to be one of the most promising candidate cathode materials for LIB [6,7]. This material attracts significant interests because the combination of nickel, manganese and cobalt provides higher reversible capacity, better cycle performance, lower cost and less toxicity compared with $LiCoO_2$ [8,9].

Selecting an appropriate method to prepare $Li[Ni_{1/3}Co_{1/3}Mn_{1/3}]O_2$ is very critical [10]. Many methods such as the solid state synthesis [11], the sol–gel method [12], the coprecipitation method [13,14], the molten salt method [15], etc., have been developed to prepared $Li[Ni_{1/3}Co_{1/3}Mn_{1/3}]O_2$. Among these methods, coprecipitation has been widely adopted as the preferred method, because it allows for a better cationic distribution control and ease of handling [16,17]. However, the mixed transition-metal hydroxide precursor is unstable during the hydroxide coprecipitation process. $Mn(OH)_2$ can easily be oxidized to MnOOH or MnO_2 after it segregated from the mixed transition-metal hydroxide [18]. Therefore, carbonate coprecipitation has been employed to prepare a stable precursor. During the carbonate coprecipitation process, the oxidation states of the transition metals are kept constant (equal to 2), which results in a homogeneous precursor of $[Ni_{1/3}Co_{1/3}Mn_{1/3}]CO_3$ [10,19].

The physical and chemical performance of the $[Ni_{1/3}Co_{1/3}Mn_{1/3}]CO_3$ precursor and the resulting $Li[Ni_{1/3}Co_{1/3}Mn_{1/3}]O_2$ product depends on the kinds of carbonate precipitator. Therefore, it is critical to investigate the effects of carbonate precipitator on the characteristics of $Li[Ni_{1/3}Co_{1/3}Mn_{1/3}]O_2$. In this study, three precipitators including Na_2CO_3, $(NH_4)_2CO_3$ and NH_4HCO_3 are employed to prepare $Li[Ni_{1/3}Co_{1/3}Mn_{1/3}]O_2$ via the carbonate coprecipitation method. The morphological, structural and electrochemical characteristics of the precursors and final products are compared in detail.

* Corresponding author. Tel.: +86 451 88060570.
** Corresponding author. Tel.: +86 451 82589186.
E-mail addresses: chaodeng2008@yahoo.cn (C. Deng), senzhang@hrbeu.edu.cn (S. Zhang).

0925-8388/$ – see front matter © 2010 Elsevier B.V. All rights reserved.
doi:10.1016/j.jallcom.2010.10.027

2. Experimental

2.1. Synthesis of precursor

The precursors were prepared by using Na_2CO_3, $(NH_4)_2CO_3$ and NH_4HCO_3 as precipitator in the following manner. An aqueous solution of $NiSO_4$, $CoSO_4$, and $MnSO_4$ (cationic ratio of Ni:Co:Ni = 1:1:1) was pumped into a continuous stirred tank reactor. At the same time, the solution of the precipitator, i.e. Na_2CO_3, $(NH_4)_2CO_3$ or NH_4HCO_3 was also separately fed into the reactor. The pH value of the coprecipitation solution was maintained via carefully controlling the addition speed of the solutions. The coprecipitation system was maintained at 40 °C with continuous stirring for 12 h. The precipitated powders were filtered and washed, and then they were dried in a vacuum oven at room temperature for 12 h.

2.2. Synthesis of $Li[Ni_{1/3}Co_{1/3}Mn_{1/3}]O_2$

The obtained precursors were pressed into pellets. The pellets were calcined at 500 °C for 5 h and were subsequently ground. The obtained powder was mixed with different amount of LiOH (the molar ratio of Li:(Mn + Co + Ni) is 1.10) using a ball mill. Finally, Pellets were remade and then calcinated at 850 °C for 12 h in air.

2.3. Measurements

Powder X-ray diffraction (XRD) employing Cu Kα radiation was used to identify the crystalline phase of the prepared powders. The surface morphology was observed with a scanning electron microscope (SEM). The chemical composition was determined with atomic absorption spectroscopy (AAS, PE, Analyst-100), which suggests that the compositions of the products coincide with the designed values. The particle size distribution was measured by Mastersizer (Malvern).

Electrochemical measurements were performed using a 2032 coin-cell composed of $Li[Ni_{1/3}Co_{1/3}Mn_{1/3}]O_2$ cathode and a lithium metal anode separated by a microporous polyethylene film. Cathode electrode was prepared by mixing the active material with conductive carbon black and Polyvinylidene Fluoride (PVDF) in a weight ratio of 80:10:10. The mixture was pressed onto an aluminum foil and then dried under vacuum at 70 °C for 10 h. Then the electrode was rolled, and the electrode circle was cut off. The laboratory cell was assembled in an argon-filled glove box, and the electrolyte consists of 1 M $LiPF_6$ – Ethylene carbonate (EC)/Dimethyl carbonate (DMC)(1:1 v/v). The electrochemical properties were measured with BTS-2000 Neware Battery Testing System, and the cells were tested at 32 mA g^{-1} between 2.8 to 4.3 V.

3. Results and discussion

In the carbonate co-precipitation process, many factors can affect the characteristics of the prepared precursors, such as the pH value, precipitator, chelating agent, reaction time, and calcinations temperature, etc. [20]. In our work, the pH value of the solution, the reaction time and the reaction temperature was fixed

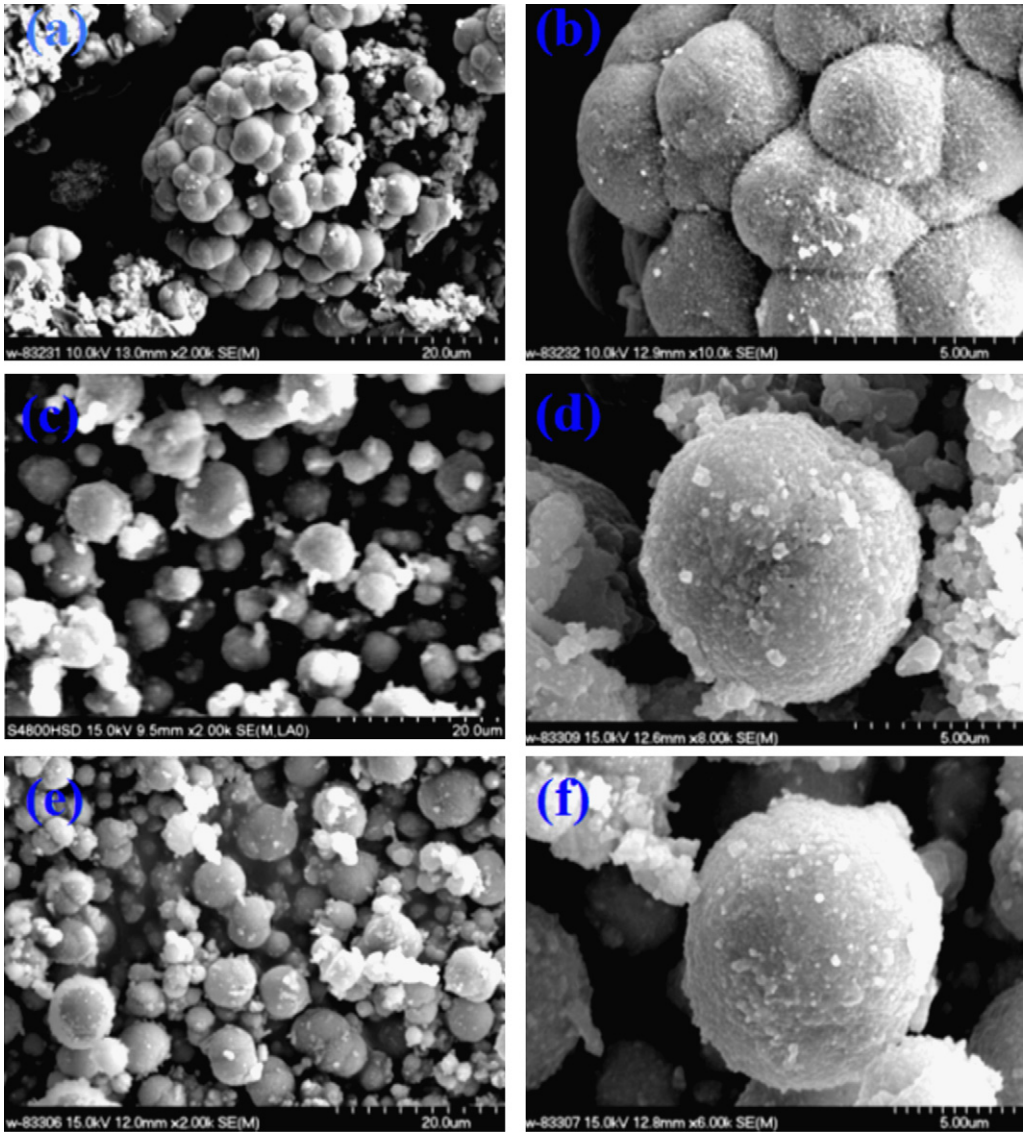

Fig. 1. SEM images of precursors prepared with different precipitators via the carbonate coprecipitation method. (a and b – precursor A; c and d – precursor B; e and f – precursor C).

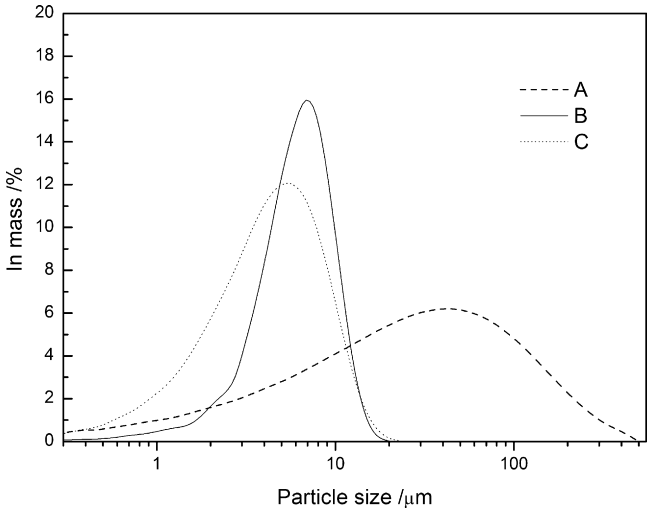

Fig. 2. Particle size distribution of precursors prepared with different precipitators via the carbonate coprecipitation method.

at 7.5, 12 h, and 40 °C, respectively. However, the precipitator was switched among Na_2CO_3, $(NH_4)_2CO_3$ and NH_4HCO_3. Under these conditions, the morphological and structural characteristics of the precursors are mainly determined by the precipitator.

Fig. 1 shows the morphological characteristics of the precursors prepared with different precipitators. For simplicity, the precursors prepared with NH_4HCO_3, $(NH_4)_2CO_3$, and Na_2CO_3 precipitators are referred as precursor A, B and C respectively. Precursor A exhibits spherical particles with the diameter of 3–4 μm. Many precursor particles closely aggregate together and form large quasi-spherical agglomerates (as shown in Fig. 1(a) and (b)). Precursor B and C exhibit spherical particles and the diameters of the particles for both samples are about 6 μm (as shown in Fig. 1(c)–(f)). Fig. 2 shows the particle size distributions of the precursors prepared with different precipitators. Precursor B has a narrower particle size distribution than precursor C, which indicates the particles of precursor B are more uniform than those of precursor C.

The structures of the prepared precursors are shown in Fig. 3. All the precursors have typical XRD patterns corresponding to $MnCO_3$, which can be indexed on the basis of the hexagonal structure in a space group of *R*3*c* [18]. However, an impurity peak near 11° (marked with asterisk) is observed for sample A, which is coincided with the characteristic of the hydrotalcite-like type compounds [21–24]. Therefore, the secondary phase can be attributed to the hydrotalcite-like compounds, such as hydroxide–carbonate mixture with multiple crystal water (e.g. $[Ni_{1/3}Co_{1/3}Mn_{1/3}](OH)_x(CO_3)_y{\cdot}zH_2O$).

Based on the above results, precursor B exhibits more uniform spherical particles than precursor C. The improved morphological characteristics can be attributed to the ammonia group in the $(NH_4)_2CO_3$ precipitator. During the coprecipitation process, ammonia acts as a chelating agent, which promotes the homogeneous growth of the precursor. Therefore, better electrochemical performance is expected for this sample. However, precursor A has special morphology and some impurity, which may be attributed to the bicarbonate (HCO_3^-) group in the NH_4HCO_3 precipitator. The bicarbonate group is a kind of zwitterionic group and it will produce carbonic group (CO_3^{2-}) through the ionization reaction (Eq. (1)) or carbonate acid (H_2CO_3) through the hydrolytic reaction (Eq. (2)).

$$HCO_3^- \rightarrow CO_3^{2-} + H^+ \quad (1)$$

$$HCO_3^- + H_2O \rightarrow H_2CO_3 + OH^- \quad (2)$$

In our case, both the ionization reaction and the hydrolytic reaction take place, and the carbonic group and carbon dioxide are produced simultaneously. The carbon dioxide is absorbed onto the particles by surface tension and easily induces aggregation, which prohibits the growth of the particles and leads to the special morphology of precursor A. The impurity in precursor A can be attributed to the reaction of transition metal ion (M^{2+}) with hydroxide group (OH^-), which is a side product of hydrolytic reaction (Eq. (2)). As to sample B and C, the CO_3^{2-} reacts with the transition metal ion (M^{2+}) directly and then the precursor is precipitated out. Therefore, the hydrolytic reaction of CO_3^{2-} is very weak and the amount of OH^- is very small. So there are no impurities in sample B and C.

The precursors are precalcined at 500 °C and the structures of the products are shown in Fig. 4. For simplicity, the precalcination products are referred as sample A, B and C. The structures of all the samples change to spinel structure corresponding to Co_3O_4, which can be indexed on the cubic spinel structure with a space group of *Fd*3*m*[10,18]. No secondary phase is observed for sample A, which can be attributed to the

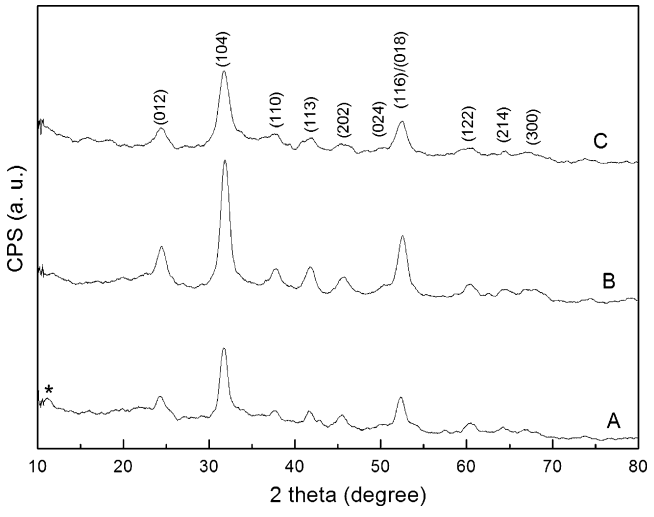

Fig. 3. XRD patterns of precursors prepared with different precipitators via the carbonate coprecipitation method. (A – precursor A; B – precursor B; C – precursor C).

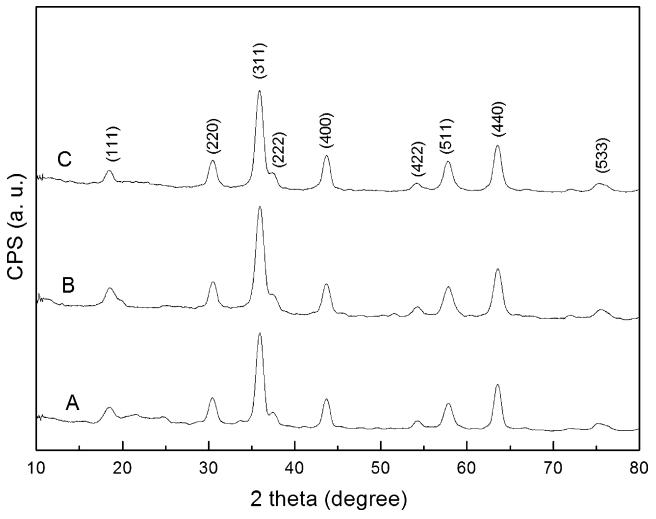

Fig. 4. XRD patterns of products obtained after precalcinations of the prepared precursors at 500 °C. (A – sample A; B – sample B; C – sample C).

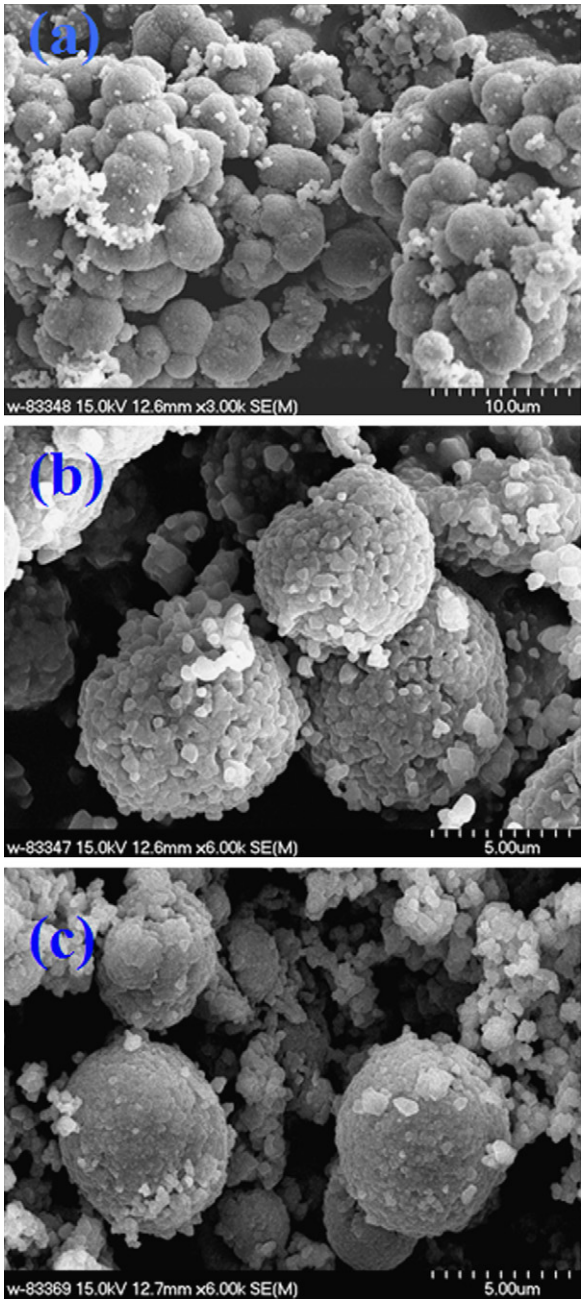

Fig. 5. SEM images of $LiNi_{1/3}Co_{1/3}Mn_{1/3}O_2$ prepared with different kinds of precipitators via the carbonate coprecipitation. (A – product A; B – product B; C – product C).

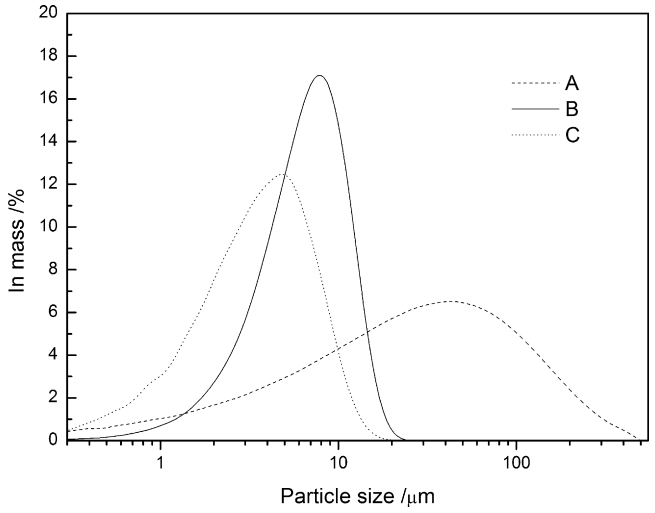

Fig. 6. Particle size distribution of precursors prepared with different precipitators via the carbonate coprecipitation method.

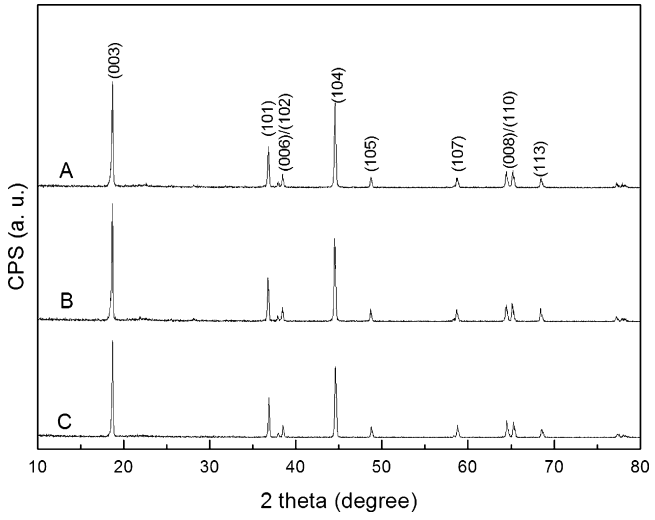

Fig. 7. XRD patterns of $Li[Ni_{1/3}Co_{1/3}Mn_{1/3}]O_2$ prepared with different kinds of precipitators via the carbonate coprecipitation method. (A – product A; B – product B; C – product C).

decomposition of the impurities, i.e. hydrotalcite-like compounds (e.g. $[Ni_{1/3}Co_{1/3}Mn_{1/3}](OH)_x(CO_3)_y{\cdot}zH_2O$), during the precalcination process.

The precalcination product was then mixed with LiOH, and the final products, i.e. $Li[Ni_{1/3}Co_{1/3}Mn_{1/3}]O_2$, were obtained after the mixture was calcined at 850 °C. The images of the final products are shown in Fig. 5. For simplicity, the final products, i.e. $Li[Ni_{1/3}Co_{1/3}Mn_{1/3}]O_2$, are referred as products A, B and C. All the samples display similar morphology to their precursors. Products B and C exhibit spherical particles with the diameters of 6 μm. Product A still has quasi-spherical union with closely aggregated particles, which is similar to its precursor. The particle size distributions of all the products are shown in Fig. 6. Product B has a narrower particle size distribution than product C, which suggests that the particles of product B are more uniform than those of product C.

The XRD patterns of the prepared $Li[Ni_{1/3}Co_{1/3}Mn_{1/3}]O_2$ are shown in Fig. 7. All the synthesized materials have typical hexagonal α-$NaFeO_2$ structure (space group: 166, *R*-3*m*) and no secondary phase is observed in the figure. The clear peak splits of (0 0 6)/(1 0 2) and (0 1 8)/(1 1 0) indicate the highly ordered layered structure of $Li[Ni_{1/3}Co_{1/3}Mn_{1/3}]O_2$ prepared with different precipitators. The lattice parameters are calculated from the XRD data and the results are summarized in Table 1. The integrated intensity ratio of I_{003}/I_{104} (*R*) is sensitive to cation mixing, thus it is often used to measure

Table 1
Lattice parameters of $LiNi_{1/3}Co_{1/3}Mn_{1/3}O_2$ prepared with different kinds of precipitators via carbonate coprecipitation.

Sample	*a* (Å)	*c* (Å)	*c*/*a*	*V* (Å)^3	$R_{I(003)/I(104)}$
A	2.8628	14.2347	4.972	101.03	1.248
B	2.8604	14.2424	4.979	100.92	1.419
C	2.8566	14.2161	4.977	100.47	1.372

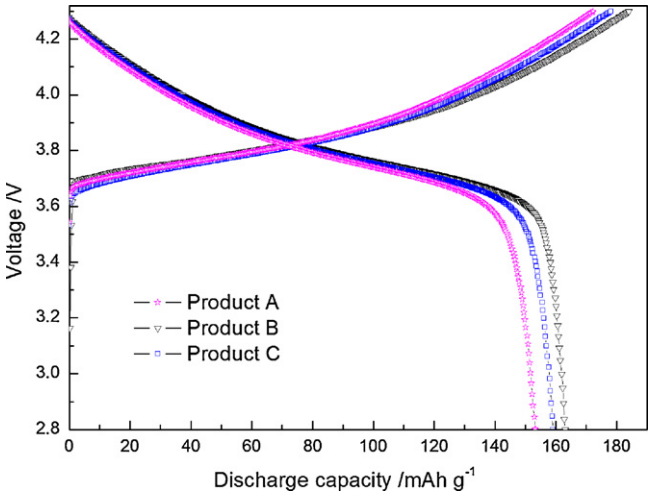

Fig. 8. Initial charge/discharge curves of $Li(Ni_{1/3}Co_{1/3}Mn_{1/3})O_2$ cathodes prepared with different precipitators. (A – product A; B – product B; C – product C).

the amount of cation mixing in the layered structure [25]. Higher *R* value is desirable for lower amount of the cation mixing [26]. Product B exhibits the highest *R* value among the samples, indicating the best crystallization and lowest cation mixing. The ratio of *c*/*a* is also an important parameter, which is related to the hexagonal structure disorder. For layered compounds, higher *c*/*a* ratio is desirable for better hexagonal structure [27]. Product B exhibits higher *c*/*a* value than the others, which reveals its better hexagonal layered structure than the others. However, product A displays the lowest *R* value and *c*/*a* ratio, which implies that its structure is the farthest from the ideal hexagonal structure.

The structural and morphological characteristics of $Li[Ni_{1/3}Co_{1/3}Mn_{1/3}]O_2$ is consistent with that of the precursors. Therefore, the precipitators play an important role in determining the structural and morphological behaviors of both the precursors and the final product of $Li[Ni_{1/3}Co_{1/3}Mn_{1/3}]O_2$.

The initial charge/discharge curves of the products are presented in Fig. 8. The cells were cycled at a constant current density of 32 mA g^{-1} (0.2 C) between 2.8 and 4.3 V (vs. Li/Li^+). The initial discharge capacities of products A, B and C are 153.2 mAh g^{-1}, 162.8 mAh g^{-1}, 159.3 mAh g^{-1}, respectively. Product B displays somewhat higher capacity than the others. The cycling performances of the samples are displayed in Fig. 9. All the materials exhibit stable cycle property, and the capacity retention of product B (93.6%) and C (91.8%) are higher than that of product A (85.8%).

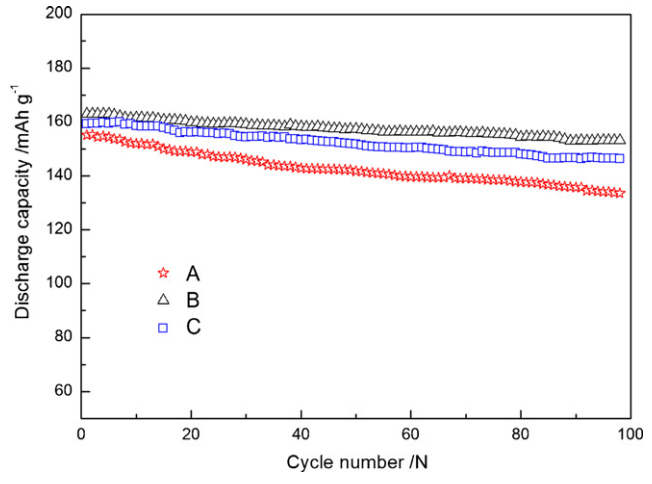

Fig. 9. Cycle performance of $Li(Ni_{1/3}Co_{1/3}Mn_{1/3})O_2$ cathodes prepared with different precipitators. (A – product A; B – product B; C – product C).

The different electrochemical performance of the $Li[Ni_{1/3}Co_{1/3}Mn_{1/3}]O_2$ can be attributed to their different structure characteristics. As discussed above, the highly ordered layered structure with low cation mixing is favorable to good electrochemical performance. In our work, better structure characteristics are obtained for product B, thus it exhibits better electrochemical properties than the others. On the contrary, product A has worse structural characteristics with higher cation mixing, which leads to its poorer electrochemical performance. Therefore, precipitator plays an important role in the carbonate coprecipitation process. It makes a great impact on the morphology, structure and electrochemical behaviors of the $Li[Ni_{1/3}Co_{1/3}Mn_{1/3}]O_2$.

4. Conclusions

Three precipitators, i.e. Na_2CO_3, $(NH_4)_2CO_3$ and NH_4HCO_3, are employed to prepare layered $Li[Ni_{1/3}Co_{1/3}Mn_{1/3}]O_2$ via the carbonate coprecipitation. The effects of the precipitators on the morphology, structure and electrochemical performance of the prepared precursors and $Li[Ni_{1/3}Co_{1/3}Mn_{1/3}]O_2$ are studied. The sample prepared by using $(NH_4)_2CO_3$ as precipitator has uniform spherical particle and good crystallinity, which results in the good electrochemical performance. The sample prepared by using Na_2CO_3 as precipitator has irregular particles and broad particle size distribution, which is due to the absence of chelating agent. Special image of big quasi-spherical union are obtained for the sample prepared by using NH_4HCO_3 as precipitator. This strange image can be attributed to the hydrolytic side reaction during the coprecipitation process, which leads to the less crystallinity and poorer electrochemical performance.

Acknowledgements

This work is supported by the National Natural Science Foundation of China (No. 50902041, 21001036), Foundation for University Key Teacher by the Heilongjiang Ministry of Education (No.1155G28), Postdoctoral Foundation of Heilongjiang Province (No. LBH-Q08057), Innovation Foundation of Harbin City (No. 2009RFQXG201) and Development Program for Outstanding Young Teachers in Harbin Normal University (No. KGB200805).

References

[1] J. Xiang, C. Chang, F. Zhang, J. Sun, J. Alloys Compd. 475 (2009) 483.
[2] G.Q. Liu, W.S. Yuan, G.Y. Liu, Y.W. Tian, J. Alloys Compd. 484 (2009) 567.
[3] K. Kang, Y.S. Meng, J. Breger, C.P. Grey, G. Ceder, Science 311 (2006) 977.
[4] A.S. Arico, P. Bruce, B. Scrosati, J.M. Tarascon, W.V. Schalkwijk, Nat. Mater. 4 (2005) 366.
[5] C. Zhu, C. Yang, W. Yang, C. Hsieh, H. Ysai, Y. Chen, J. Alloys Compd. 496 (2010) 703.
[6] R. Guo, P. Shi, X. Cheng, C. Du, J. Alloys Compd. 473 (2009) 53.
[7] C. Cheng, L. Tan, A. Hu, H. Liu, X. Huang, J. Alloys Compd. 506 (2010) 889.
[8] D.D. Macneil, Z. Lu, J.R. Dahn, J. Electrochem. Soc. 149 (2002) A1332.
[9] K.M. Shaju, G.V. Subba Rao, B.V.R. Chowdari, J. Electrochem. Soc. 151 (2004) A1324.
[10] S.H. Park, H.S. Shin, S.T. Myung, C.S. Yoon, K. Amine, Y.K. Sun, Chem. Mater. 17 (2005) 6.
[11] L. Yu, W. Qiu, F. Lian, J. Huang, X. Kang, J. Alloys Compd. 471 (2009) 317.
[12] H. Xia, H. Wang, W. Xiao, L. Lu, M.O. Lai, J. Alloys Compd. 480 (2009) 696.
[13] S. Zhang, C. Deng, S.Y. Yang, H. Niu, J. Alloys Compd. 484 (2009) 519.
[14] C. Deng, S. Zhang, B.L. Fu, S.Y. Yang, L. Ma, J. Alloys Compd. 496 (2010) 521.
[15] K. Du, Z.D. Peng, G.R. Hu, Y.N. Yang, L. Qi, J. Alloys Compd. 476 (2009) 329.
[16] Y. Fujii, H. Miura, N. Suzuki, T. Shoji, N. Nakayama, J. Power Sources 171 (2007) 894.
[17] K.K. Lee, K.B. Kim, J. Electrochem. Soc. 147 (2000) 1709.
[18] S.H. Park, S.H. Kang, I. Belharouak, Y.K. Sun, K. Amine, J. Power Sources 177 (2008) 177.
[19] T.H. Cho, S.M. Park, M. Yoshio, T. Hirai, Y. Hideshima, J. Power Sources 142 (2005) 306.

[20] S. Myung, M. Lee, S. Komaba, N. Kumagai, Y. Sun, Electrochim. Acta 50 (2005) 4800.
[21] V. Gupta, S. Gupta, N. Miura, J. Power Sources 177 (2008) 685.
[22] X.F. Zhang, Z.Y. Wen, X.J. Zhu, B. Lin, J.C. Zhang, S.H. Huang, Mater. Lett. 60 (2006) 1470.
[23] F. Kovanda, T. Grygar, V. Dornicak, Solid State Sci. 5 (2003) 1019.
[24] N.V. Kosova, E.T. Devyatkina, V.V. Kaichev, J. Power Sources 174 (2007) 735.
[25] Z.L. Liu, A.S. Yu, J.Y. Lee, J. Power Sources 81–82 (1999) 416.
[26] J.N. Reimers, E. Rossen, C.D. Jones, J.R. Dahn, Solid State Ionics 67 (1990) 123.
[27] X. Zhang, Z. Wen, X. Yang, X. Xu, J. Li, Mater. Res. Bull. 41 (2006) 662.